ELSEVIER

Engineering Analysis with Boundary Elements 31 (2007) 994–1002

ENGINEERING ANALYSIS with BOUNDARY ELEMENTS

www.elsevier.com/locate/enganabound

Eigenvalue and eigenfunction analysis arising from degenerate scale problem of BIE in plane elasticity

Y.Z. Chen*, Z.X. Wang, X.Y. Lin

Division of Engineering Mechanics, Jiangsu University, Zhenjiang, Jiangsu 212013, PR China

Received 23 August 2006; accepted 21 May 2007
Available online 24 October 2007

Abstract

A new boundary integral equation (BIE) of plane elasticity is suggested with the use of a novel kernel. The relevant homogenous equation is also suggested. The equation is studied in a discrete form, or it is reduced to an algebraic equation. From the condition that the value of a determinant vanishes, the degenerate scale (or the eigenvalue) and the non-trivial solution (or the eigenfunction) are obtained approximately. Except for the notch with symmetric configuration for two axes, computed results prove that there are two degenerate scales in general. The dependence of the eigenvalue and eigenfunction with respect to the translation or the rotation of notch is investigated. It is found that the eigenvalues are invariant with respect to the translation and the rotation of notch. However, the eigenfunctions are changed when the notch has a rotation. Several numerical examples that include a rectangular notch, a half-ring-shaped notch and a complicated notch configuration are presented with the computed eigenvalues and eigenfunctions.

Keywords: Boundary integral equation; Exterior boundary value problem; Degenerate scale; Eigenvalue; Non-trivial solution; Eigenfunction

1. Introduction

The boundary integral equation (abbreviated as BIE) was widely used in elasticity, and the fundamental for BIE could be found [1–3]. Heritage and early history of the boundary element method was summarized more recently [4]. However, some difficult points for the BIE in plane elasticity remain. For example, engineers may not be aware of the risk in BIE computation when a degenerate scale occurs.

It is well known that the special geometry size may result in a non-unique solution for potential problem (Laplace equation), and the size is called the degenerate scale. Alternatively speaking, for relevant homogenous BIE, there is a non-trivial solution. Below, the degenerate scale is called the eigenvalue, and the non-trival solution is called the eigenfunction. The degenerate scale problem for potential problem (Laplace equation) was studied for a circular region [5,6]. The same problem for a circular bending plate was investigated [7].

In the case of plane elasticity, the degenerate scale problem in BIE still exists. For example, if the conventional boundary integral equation (abbreviated as CBIE) is used for a ring region with the vanishing displacements along the boundary, in some particular geometry conditions the corresponding homogenous equation has non-trivial solution for the boundary tractions [8–10]. In fact, if the displacements are vanishing at the boundary of ring region, the stresses must be equal to zero. Therefore, the obtained result seriously violates the basic property of elasticity.

For the degenerate scale problems, investigators paid attention to some regular boundaries, for example, the boundary of the circular region or the ring region. It is felt that less attention was paid to the numerical method for the problems with arbitrary boundary configuration.

The merit of the degenerate scale problem is compactly introduced below. Without losing generality, the elliptic notch in an infinite plate can be taken as an example (Fig. 1).

*Corresponding author.

0955-7997/$ - see front matter © 2007 Published by Elsevier Ltd.
doi:10.1016/j.enganabound.2007.05.003

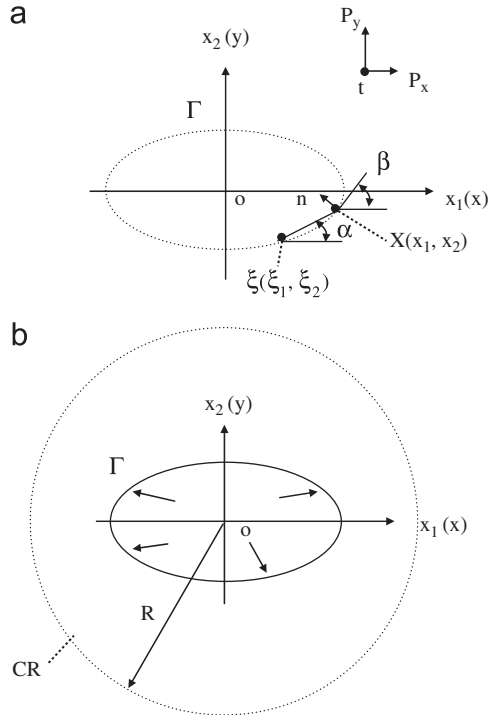

Fig. 1. (a) A concentrated force applied at the point $z = t$, or the loading condition for the fundamental stress field, (b) some loadings having resultant forces applied on the elliptic contour, or the loading condition for a stress field.

The ellipse has two half-axes "a" and "b". Assume that the ratio b/a is given beforehand. Therefore, the size "a" will fully determine the configuration of ellipse. Let the boundary displacement to be equal to zero, a homogeneous BIE is obtained [3]

$$\int_{\Gamma} U_{ij}^{*}(\xi, x, a) p_j(x)\, \mathrm{d}s(x) = 0, \quad (i = 1, 2, \ \ \xi \in \Gamma), \tag{1}$$

where Γ is the boundary of the notch, $\xi \in \Gamma$ is the source point, and $x \in \Gamma$ is the field point, and $p_j(x)$ $(j = 1, 2)$ denote the applied tractions along the boundary. Meantime, the kernel $U_{ij}^{*}(\xi, x, a)$ can be found in textbook. It is preferable to write the kernel U_{ij}^{*} in the form $U_{ij}^{*}(\xi, x, a)$, where the size a is involved. The kernel $U_{ij}^{*}(\xi, x, a)$ may depend on the Poisson's ratio v. However, this is not an essential point in analysis.

Clearly, Eq. (1) has a trivial solution $p_j(x) = 0$ $(j = 1, 2)$, and this solution is not interesting. In the degenerate scale problem, it is desirable to find some particular values of "a" such that Eq. (1) has non-trivial solution. For the elliptic notch case, it is pointed out later that there are two particular values $a = \lambda_1$ and λ_2 such that Eq. (1) has two non-trivial solutions: (a) $p_1(x) \neq 0$, $p_2(x) = 0$ for $a = \lambda_1$ case and (b) $p_1(x) = 0$, $p_2(x) \neq 0$ for $a = \lambda_2$ case, respectively.

Except for the circular hole case, it is seen that the degenerate scale problem cannot be solved in a closed form. Therefore, the degenerate scale problem should generally be solved by using a numerical technique.

In this paper, a new kernel $U_{ij}^{*1}(\xi, x)$ in BIE of plane elasticity (a displacement representation in the fundamental field) is introduced, which satisfies the regularity condition at infinity for exterior problem in BIE [3]. A new BIE is suggested with the use of the introduced kernel $U_{ij}^{*1}(\xi, x)$. After substituting the vanishing displacement in the BIE, the relevant homogenous equation is obtained. The equation is studied in a discrete form, or it is reduced to an algebraic equation. From the condition that the value of a determinant vanishes, the degenerate scale (or the eigenvalue) and the non-trivial solution (or the eigenfunction) are obtained approximately.

Except for the notch with symmetric property in two directions, computed results prove that there are two degenerate scales in general. The dependence of the eigenvalue and eigenfunction with respect to the translation or the rotation of notch configuration is investigated. It is found that the eigenvalue is an invariant with respect to the translation and the rotation. However, the eigenfunction is changed when the notch configuration has a rotation. Several numerical examples that include a rectangular notch, a half-ring-shaped notch and a complicated notch configuration are presented with the computed eigenvalues and eigenfunctions.

2. General analysis

The eigenvalue and eigenfunction analysis arising from degenerate scale problem of BIE in plane elasticity is studied below. Two kinds of formulation, one in the form of BIE, the other in the discrete form, are introduced. For clarity, the elliptic notch is chosen as an example in the following derivation, and relevant computed results are presented.

2.1. Formulation of the eigenvalue and eigenfunction problem in the form of a BIE

Without losing generality, we can introduce the BIE for the region between the elliptic contour Γ and a large circle "CR" (Fig. 1). The observation point ξ is assumed on the elliptic contour $\xi \in \Gamma$. For the plane strain case, the suggested BIE can be written as follows [3]:

$$\frac{1}{2} u_i(\xi) + \int_{\Gamma} P_{ij}^{*}(\xi, x) u_j(x)\, \mathrm{d}s(x) = \int_{\Gamma} U_{ij}^{*1}(\xi, x) p_j(x)\, \mathrm{d}s(x) + D_1(CR), \quad (i = 1, 2, \ \ \xi \in \Gamma), \tag{2}$$

where $u_j(\xi)$, $u_j(x)$ are the displacements, and $p_j(x)$ $(j = 1, 2)$ denotes the applied tractions along the boundary. In Eq. (2), $D_1(CR)$ is a mutual work difference integral (abbreviated as MWDI) on a large circle CR and is

defined by

$$D_1(CR) = -\int_{CR} P^*_{ij}(\xi,x)u_j(x)\,\mathrm{d}s(x) + \int_{CR} U^{*1}_{ij}(\xi,x)p_j(x)\,\mathrm{d}s(x), \quad (3)$$

and the kernel $P^*_{ij}(\xi,x)$ is defined by [3]

$$P^*_{ij}(\xi,x) = -\frac{1}{4\pi(1-v)}\frac{1}{r}\{(r_{,1}n_1 + r_{,2}n_2)((1-2v)\delta_{ij} + 2r_{,i}r_{,j}) + (1-2v)(n_i r_{,j} - n_j r_{,i})\}, \quad (4)$$

where v is the Poisson's ratio. In Eq. (4), the Kronecker deltas δ_{ij} is defined as $\delta_{ij}=1$ for $i=j$, $\delta_{ij}=0$ for $i\neq j$, and

$$r^2 = (x_1-\xi_1)^2 + (x_2-\xi_2)^2,\ \ r_{,1} = \frac{x_1-\xi_1}{r} = \cos\alpha,$$
$$r_{,2} = \frac{x_2-\xi_2}{r} = \sin\alpha,\ \ n_1 = -\sin\beta,\ \ n_2 = \cos\beta, \quad (5)$$

where the angles α and β are indicated in Fig. 1(a).

The kernel $P^*_{ij}(\xi,x)$ can be obtained in a usual way [3]. The kernel $U^{*1}_{ij}(\xi,x)$ may be obtained from a fundamental stress field (Fig. 1(a)). It is known that the kernel $U^{*1}_{ij}(\xi,x)$ is a displacement field caused by concentrated forces applied at some point in the infinite medium. Therefore, the adopted kernels for $U^{*1}_{ij}(\xi,x)$ can be differed each other by a constant. It is proved that if a particular displacement from fundamental stress field is used, we can obtain $D_1(CR)=0$ and the relevant kernel $U^{*1}_{ij}(\xi,x)$ takes the following form (see Appendix A)

$$U^{*1}_{ij}(\xi,x) = H\{(3-4v)\ln(r)\delta_{ij} - r_{,i}r_{,j} + 0.5\delta_{ij}\},$$
$$\text{with}\ \ H = -\frac{1}{8\pi(1-v)G}, \quad (6)$$

where G denotes the shear modulus of elasticity. The condition $D_1(CR)=0$ was named the regularity condition in literature [3]. Since this condition ($D_1(CR)=0$) is satisfied for the suggested fundamental solution, Eq. (2) can be reduced to the following BIE

$$\frac{1}{2}u_i(\xi) + \int_\Gamma P^*_{ij}(\xi,x)u_j(x)\,\mathrm{d}s(x) = \int_\Gamma U^{*1}_{ij}(\xi,x)p_j(x)\,\mathrm{d}s(x),$$
$$(i=1,2,\ \ \xi\in\Gamma). \quad (7)$$

From the above it is seen that only if $U^{*1}_{ij}(\xi,x)$ takes the form of Eq. (6), Eq. (2) can be reduced to Eq. (7). Otherwise, a term $D_1(CR)$ in Eq. (2) will make the BIE more complicated.

It is preferable to write the kernel $U^{*1}_{ij}(\xi,x)$ in the form $U^*_{ij}(\xi,x,a)$, where a size a is involved. We take an elliptic notch with two half-axes a and b as an example. In addition, for example, $b/a=0.5$ is assumed. In this case, the value of a will solely determine the size of the elliptic notch; it in turn will be a parameter in the kernel $U^{*1}_{ij}(\xi,x,a)$.

If we assume $u_j(\xi)=0$ ($j=1,2,\ \xi\in\Gamma$) in the left side of Eq. (7), the following homogenous integral equation is obtained:

$$\int_\Gamma U^{*1}_{ij}(\xi,x,a)p_j(x)\,\mathrm{d}s(x) = 0\ \ (i=1,2,\ \ \xi\in\Gamma). \quad (8)$$

Clearly, the homogenous BIE (8) has a trivial solution $p_j(x)=0$ ($j=1,2,\ \xi\in\Gamma$), which is of no interest. In the case of a circular hole notch, it was proved that there is a particular value for the size a, for which a non-trivial solution exists, or $p_j(x)\neq 0$ ($j=1,2,\ x\in\Gamma$). This particular value a is an eigenvalue for the homogenous equation, and $p_j(x)\neq 0$ ($j=1,2,\ x\in\Gamma$) are the eigenfunctions. However, it is not easy to study the problem for an arbitrary notch configuration. Therefore, the following numerical procedure is introduced.

2.2. Formulation of the eigenvalue and eigenfunction problem in a discrete form

Without losing generality, the elliptic notch in infinite plate is taken as an example (Fig. 2(a)). From a real computation, it is found that there are two eigenvalues $a=\lambda_{1,\text{exact}}$ and $\lambda_{2,\text{exact}}$. In the numerical technique, the ellipse is divided into 120 intervals, and $v=0.3$ is assumed. The constant traction is assumed for each interval. After making discretization, Eq. (8) may be written in the following form:

$$\sum_{n=1}^{M} U_{mn}\tilde{p}_n = 0,\ \ (m=1,2,\ldots,M), \quad (9)$$

where the matrix U_{mn} ($m,n=1,\ldots,M$) is derived from the kernel function $U^{*1}_{ij}(\xi,x,a)$, and $\tilde{p}_n$ denotes the loading vector that is assumed on the intervals. The vector $\tilde{p}_n$ is composed of $p_{1(i)}$, $p_{2(i)}$ ($i=1,2,\ldots$), which are tractions on intervals. Eq. (9) may be written in a matrix form as follows:

$$\mathbf{U}\tilde{p} = 0. \quad (10)$$

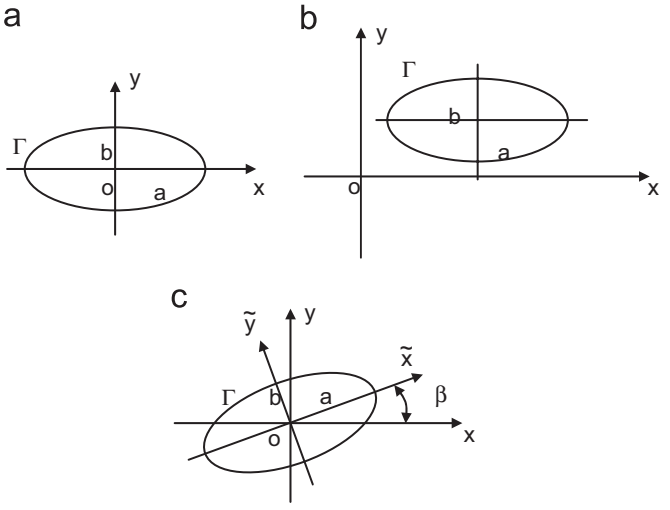

Fig. 2. (a) An elliptic notch in an infinite plate. (b) An elliptic notch with a translation from the origin of coordinates. (c) An elliptic notch with a rotation.

Table 1
Computed values of two degenerate scales for an elliptic notch: (1) $a=\lambda_1=f_1(b/a)$ and $a=\lambda_2=f_2(b/a)$ in the case of using the kernel $U_{ij}^{*1}(\xi,x,a)$ (see Eq. (12)), (2) $a=\lambda_1=g_1(b/a)$ and $a=\lambda_1=g_2(b/a)$ in the case of using the kernel $U_{ij}^{*2}(\xi,x,a)$ (see Eq. (19)), within the range $0.1\leqslant b/a\leqslant 1.0$ (see Fig. 2(a))

	b/a									
	0.1	0.2	0.3	0.4	0.5	0.6	0.7	0.8	0.9	1.0
f_1	2.282780	2.006306	1.787181	1.609634	1.463102	1.340271	1.235928	1.146265	1.068437	1.000284
f_2	1.448964	1.385311	1.325109	1.268597	1.215765	1.166471	1.120510	1.077648	1.037649	1.000284
g_1	3.013710	2.648710	2.359424	2.125027	1.931576	1.769417	1.631664	1.513290	1.410544	1.320568
g_2	1.912902	1.828878	1.749399	1.674793	1.605044	1.539967	1.479289	1.422702	1.369897	1.320568

The degenerate scale a (or the eigenvalue) is evaluated from the following equation:

$$\det(\mathbf{U})=0. \tag{11}$$

In a real computation, the degenerate scale a is evaluated by the following technique. A sufficient small value δ is assumed in advance ($\delta=1\times10^{-6}$ is used in this paper). Once we find a value for λ such that $\det(U)|_{a=\lambda-\delta}>0$ and $\det(U)|_{a=\lambda+\delta}<0$ (or $\det(U)|_{a=\lambda-\delta}<0$ and $\det(U)|_{a=\lambda+\delta}>0$), the degenerate scale $a=\lambda$ is obtained approximately.

For the ratio b/a within the range $0.1<b/a<1$, two degenerate scales $a=\lambda_1$ and λ_2 were found from the computation. In the case of using the kernel $U_{ij}^{*1}(\xi,x,a)$, the obtained degenerate scales are expressed as

$$\lambda_1=f_1(b/a),\quad \lambda_2=f_2(b/a). \tag{12}$$

The computed results for $f_1(b/a)$, $f_2(b/a)$ are listed in Table 1. It can be seen from the tabulated results that, when $b/a=1$ the two degenerate scales are merged into one value $a=\lambda_1=\lambda_2=1.000284$, or this is the case of double roots. Meantime, the exact one takes the value $a=\lambda_{1,\text{exact}}=\lambda_{2,\text{exact}}=1$.

The $b/a=0.5$ case is taken as an example to find the non-trivial solution for $\tilde{p}_n$. Using the mentioned technique, two degenerate scales, $a=\lambda_1=1.463102$ and $a=\lambda_2=1.215765$ (for $b/a=0.5$ case), have been achieved approximately. The non-trivial solution for $\tilde{p}_n$ can be found in the following way. After taking $a=\lambda_1=1.463102$, we can formulate the matrix $\mathbf{U}$ with the elements U_{mn} $(m,n=1,\ldots,M)$. Substituting $\tilde{p}_1=1$ in Eq. (9) yields

$$\sum_{n=2}^{M}U_{mn}\tilde{p}_n=-U_{m1}\quad(m=1,2,\ldots,M). \tag{13}$$

We may truncate $M-1$ equations from Eq. (13), and obtain

$$\sum_{n=2}^{M}U_{mn}\tilde{p}_n=-U_{m1}\quad(m=2,\ldots,M). \tag{14}$$

From Eq. (14), we can obtain a solution for $\tilde{p}_n$ $(n=2,3,\ldots,M)$. Obviously, the obtained values $\tilde{p}_n$ $(n=1,2,3,\ldots,M)$ are composed from values of two functions $p_1(\theta)$ and $p_2(\theta)$ at the discrete points. In the case of assuming $p_1^2(\theta)+p_2^2(\theta)|_{\theta=0^\circ}=1$, two functions $p_1(\theta)$ and $p_2(\theta)$ can be obtained immediately. The computed results for tractions are expressed as follows:

$$p_1=p_1(\theta),\quad p_2=p_2(\theta)$$
$$\text{(tractions at the boundary points, } x=a\cos\theta,\quad y=b\cos\theta). \tag{15}$$

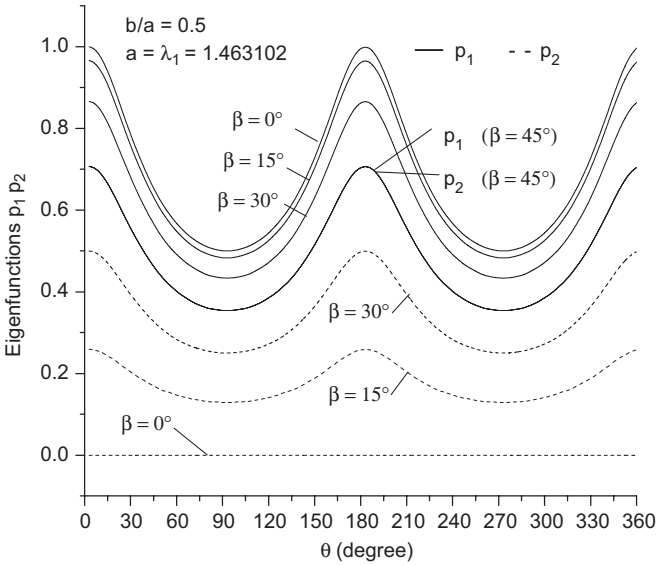

Fig. 3. Eigenfuctions $p_1(\beta,\theta)$, $p_2(\beta,\theta)$ for an elliptic notch with $b/a=0.5$ in the case of eigenvalue $a=\lambda_1=1.463102$ (β the rotation angle of the notch, see Fig. 2(c) and Eq. (17)).

Both functions $p_1(\theta)$ and $p_2(\theta)$ are plotted in Fig. 3 (the $\beta=0^\circ$ case). From computed results, it is found that $p_2(\theta)=0.000$. That is to say, the degenerate scale $a=\lambda_1=1.463102$ only gives the component p_1 the non-trivial solution.

One important point in this study is about the dependence of eigenvalues and eigenfunctions with respect to the location of the ellipse. In the first condition, the elliptic notch has a translation (Fig. 2(b)). In this case, from the structure of the kernel $U_{ij}^{*1}(\xi,x,a)$, it is seen that the

eigenvalues and the eigenfunctions are invariants with respect to the translation of ellipse.

In the second condition, the elliptic notch has a rotation (Fig. 2(c)). In this case, we have to consider three cases:

(a) Evaluation of eigenfunctions in ox_1x_2 coordinates with no rotation of the ellipse notch (Fig. 2(a)).
(b) Evaluation of eigenfunctions in $o\tilde{x}_1\tilde{x}_2$ coordinates with a rotation β of the ellipse notch (Fig. 2(c)).
(c) Evaluation of eigenfunctions in ox_1x_2 coordinates with a rotation β of the ellipse notch (Fig. 2(c)).

In the three cases, same numbering for the discretization was used. Clearly, the eigenvalues and eigenfunctions must be the same for the cases (a) and (b).

Numerical evaluation proves that the eigenvalues in the case (c) are same as in the case (a). However, this conclusion is not easy to prove theoretically. Two ways can be used to evaluate the eigenfunctions in the case (c). In the first way, the eigenfunctions are directly obtained from the computation as mentioned above. In the second way, we first obtain the eigenfunctions for case (b), and denote them as p_{1r} and p_{2r}.

Further, the eigenfuctions for the case (c) can be evaluated by

$$p_1 = p_{1r}\cos\beta - p_{2r}\sin\beta,\quad p_2 = p_{1r}\sin\beta + p_{2r}\cos\beta. \tag{16}$$

It is found that the results obtained from two ways coincide. Similar to Eq. (15), the eigenfunctions for the case (c) are expressed as

$$p_1 = p_1(\beta,\theta),\quad p_2 = p_2(\beta,\theta)$$
(tractions at the boundary points, $x = a\cos\theta$, $y = b\cos\theta$). (17)

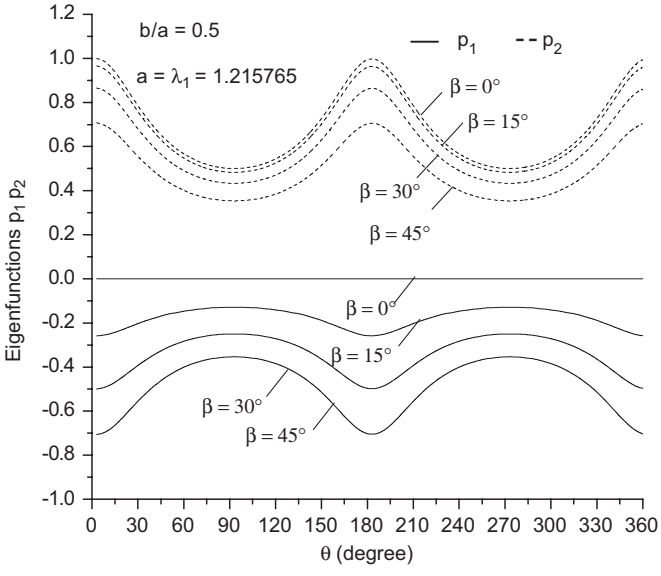

Fig. 4. Eigenfuctions $p_1(\beta,\theta)$, $p_2(\beta,\theta)$ for an elliptic notch with $b/a = 0.5$ in the case of eigenvalue $a = \lambda_2 = 1.215765$ (β the rotation angle of the notch, see Fig. 2(c) and Eq. (17)).

Under the following conditions: (a) $v = 0.3$, (b) $b/a = 0.5$, (c) for the eigenvalue $a = \lambda_1 = 1.463102$, (d) for the rotations $\beta = 0^\circ$, 15°, 30° and 45°, the computed results are plotted in Fig. 3.

Similarly, under the following conditions: (a) $v = 0.3$, (b) $b/a = 0.5$, (c) for the second eigenvalue $a = \lambda_2 = 1.215765$, (d) for the rotations $\beta = 0^\circ$, 15°, 30° and 45°, the computed results are expressed in the form of Eq. (17), and they are plotted in Fig. 4. On contrary to the case of $a = \lambda_1 = 1.463102$ and $\beta = 0^\circ$, it is found that $p_1(\theta,\beta)|_{\beta=0^\circ} = 0.000$, $p_2(\theta,\beta)|_{\beta=0^\circ} \neq 0$ in the present case.

The other important problem is the dependence of the eigenvalue to the used kernel $U^*_{ij}(\xi,x)$. In literature, a kernel was introduced [3]

$$U^{*2}_{ij}(\xi,x) = H\{(3-4v)\ln(r)\delta_{ij} - r_i r_j\},$$
$$\text{with } H = -\frac{1}{8\pi(1-v)G}. \tag{18}$$

For the ratio b/a within the range $0.1 < b/a < 1$ and the usage of the kernel $U^{*2}_{ij}(\xi,x)$, the computed degenerate scales are expressed as

$$\lambda_1 = g_1(b/a),\quad \lambda_2 = g_2(b/a). \tag{19}$$

The computed results for $g_1(b/a)$, $g_2(b/a)$ are also listed in Table 1. It can be seen from the tabulated results that, when $b/a = 1$, the two degenerate scales are merged into one value $a = \lambda_1 = \lambda_2 = 1.320568$, or this is the case of double roots. Meantime, the exact one takes the value $a = \lambda_{1,\text{exact}} = = \lambda_{2,\text{exact}} = \exp(1/(2(3-4v)) = 1.320193$ (for $v = 0.3$) [8,9].

It is noted that the notations $\lambda_1 = f_1(b/a)$ and $\lambda_2 = f_2(b/a)$ are some eigenvalues using the kernel $U^{*1}_{ij}(\xi,x,a)$, and $\lambda_1 = g_1(b/a)$ and $\lambda_2 = g_2(b/a)$ are some eigenvalues using the kernel $U^{*2}_{ij}(\xi,x,a)$. Meantime, $p_1 = p_1(\beta,\theta)$, $p_2 = p_2(\beta,\theta)$, p_{1r} and p_{2r} denote the eigenfunctions. Those notations are also used in the following numerical examples.

3. Some numerical examples

Some numerical examples with the calculated results are presented below.

Example 3.1. The first example is devoted to a rectangle notch with width "2a" and height "2b" (Fig. 5(a)). Similar to the elliptic notch case, in the case of using the kernel $U^{*1}_{ij}(\xi,x)$ (or $U^{*1}_{ij}(\xi,x,a)$), the obtained degenerate scales are expressed as

$$\lambda_1 = f_1(b/a),\quad \lambda_2 = f_2(b/a). \tag{12a}$$

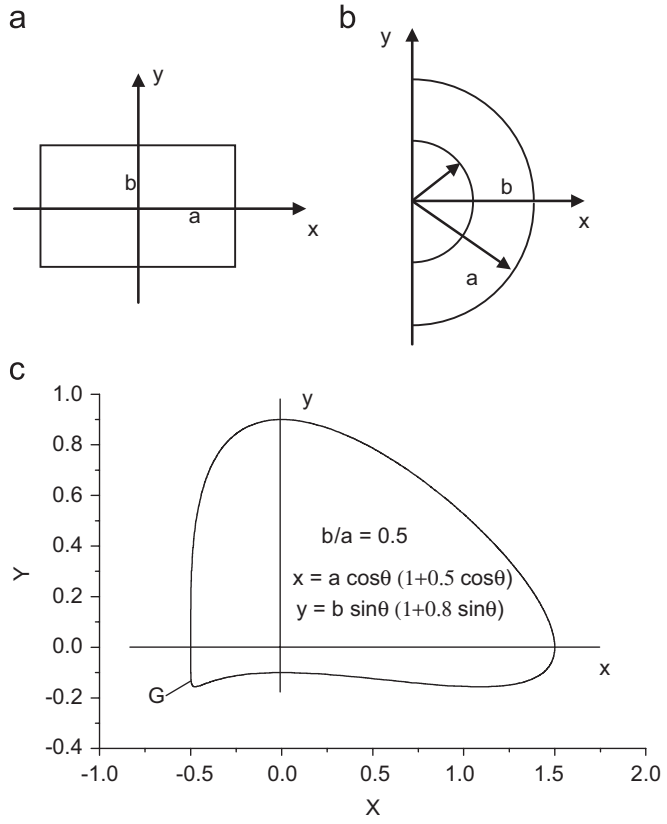

Fig. 5. (a) A rectangular notch in an infinite plate, (b) a half-ring-shaped notch in an infinite plate, (c) a notch with a complicated configuration.

Meantime, in the case of using the kernel $U_{ij}^{*2}(\xi, x)$, the obtained degenerate scales are expressed as

$$\lambda_1 = g_1(b/a), \quad \lambda_2 = g_2(b/a). \tag{19a}$$

The computed results for $\lambda_1 = f_1(b/a)$, $\lambda_2 = f_2(b/a)$, $\lambda_1 = g_1(b/a)$ and $\lambda_2 = g_2(b/a)$ are listed in Table 2. From the tabulated results, we see the following characters for the eigenvalues. Generally, the eigenvalues $g_1(b/a)$ and $g_2(b/a)$ (using the kernel $U_{ij}^{*2}(\xi, x)$) are higher than $f_1(b/a)$ and $f_2(b/a)$ (using the kernel $U_{ij}^{*1}(\xi, x)$). Secondly, if the b/a ratio is smaller, the relevant eigenvalue is higher. When $b/a \to 1$, two eigenvalues are merged into one value $a = \lambda_1 = \lambda_2 = 0.845705$ (using the kernel $U_{ij}^{*1}(\xi, x)$), or into $a = \lambda_1 = \lambda_2 = 1.116417$ (using the kernel $U_{ij}^{*2}(\xi, x)$). The eigenfunctions can also be evaluated, and they are not reported here for compactness of paper.

Example 3.2. The second example is devoted to a half-ring-shaped notch with inner radius b and outer radius a (Fig. 5(b)). Similar to the elliptic notch case, the degenerate scales are expressed as

$$\lambda_1 = f_1(b/a), \quad \lambda_2 = f_2(b/a) \quad \text{(using the kernel } U_{ij}^{*1}(\xi, x)\text{)}, \tag{12b}$$

$$\lambda_1 = g_1(b/a), \quad \lambda_2 = g_2(b/a) \quad \text{(using the kernel } U_{ij}^{*2}(\xi, x)\text{)}. \tag{19b}$$

Table 2
Computed values of two degenerate scales for a rectangular notch: (1) $a = \lambda_1 = f_1(b/a)$ and $a = \lambda_1 = f_2(b/a)$ in the case of using the kernel $U_{ij}^{*1}(\xi, x, a)$ (see Eq. (12)), (2) $a = \lambda_1 = g_1(b/a)$ and $a = \lambda_1 = g_2(b/a)$ in the case of using the kernel $U_{ij}^{*2}(\xi, x, a)$ (see Eq. (19)), within the range $0.1 \leqslant b/a \leqslant 1.0$ (see Fig. 5(a))

	b/a									
	0.1	0.2	0.3	0.4	0.5	0.6	0.7	0.8	0.9	1.0
f_1	2.071950	1.748806	1.526554	1.360652	1.230895	1.125541	1.038214	1.964331	0.900892	0.845705
f_2	1.379713	1.275461	1.191292	1.120656	1.060276	1.007059	0.960136	0.918092	0.880126	0.845705
g_1	2.735373	2.308761	2.015345	1.796323	1.625019	1.485932	1.370643	1.273103	1.189351	1.116417
g_2	1.821448	1.682714	1.572734	1.479482	1.399768	1.329512	1.267565	1.212059	1.161936	1.116417

Table 3
Computed values of two degenerate scales for a half-ring-shaped notch: (1) $a = \lambda_1 = f_1(b/a)$ and $a = \lambda_1 = f_2(b/a)$ in the case of using the kernel $U_{ij}^{*1}(\xi, x, a)$ (see Eq. (12)), (2) a $= \lambda 1 = g_1(b/a)$ and $a = \lambda_1 = g_2(b/a)$ in the case of using the kernel $U_{ij}^{*2}(\xi, x, a)$ (see Eq. (19)), within the range $0.1 \leqslant b/a \leqslant 1.0$ (see Fig. 5(b))

	b/a								
	0.1	0.2	0.3	0.4	0.5	0.6	0.7	0.8	0.9
f_1	1.406855	1.408991	1.412357	1.417432	1.423731	1.431901	1.442429	1.457500	1.480938
f_2	1.193183	1.195108	1.198271	1.202954	1.209070	1.216944	1.227236	1.241525	1.262509
g_1	1.857320	1.860139	1.864584	1.871165	1.879600	1.890385	1.904284	1.924181	1.955124
g_2	1.572232	1.577773	1.581948	1.588132	1.596206	1.606600	1.620188	1.639052	1.666755

Table 4
Computed values of two degenerate scales for a complicated notch: (1) $a=\lambda_1=f_1(b/a)$ and $a=\lambda_1=f_2(b/a)$ in the case of using the kernel $U_{ij}^{*1}(\xi,x,a)$ (see Eq. (12)), (2) a $=\lambda 1=g_1(b/a)$ and $a=\lambda_1=g_2(b/a)$ in the case of using the kernel $U_{ij}^{*2}(\xi,x,a)$ (see Eq. (19)), within the range $0.1\leqslant b/a\leqslant 1.0$ (see Eq. (20) and Fig. 5(c))

	b/a									
	0.1	0.2	0.3	0.4	0.5	0.6	0.7	0.8	0.9	1.0
f_1	2.229295	1.937519	1.713762	1.536263	1.392297	1.273760	1.175415	1.094149	1.028311	0.975819
f_2	1.431581	1.356720	1.288478	1.225788	1.167814	1.113735	1.062551	1.012859	0.962929	0.912261
g_1	2.943099	2.557899	2.262496	2.028163	1.838102	1.681609	1.551775	1.444488	1.357569	1.288269
g_2	1.889962	1.791131	1.701039	1.618276	1.541740	1.470345	1.402774	1.337169	1.271252	1.204360

The computed results for $\lambda_1=f_1(b/a)$, $\lambda_2=f_2(b/a)$, $\lambda_1=g_1(b/a)$ and $\lambda_2=g_2(b/a)$ are listed in Table 3. A particular character can be found in the present example. In this example, we see that the dependence of the eigenvalues to the ratio b/a is minor. For example, we have $f_1(b/a)|_{b/a=0.1}=1.406855$ and $f_1(b/a)|_{b/a=0.9}=1.480938$.

Example 3.3. The third example is devoted to a notch with a complicated configuration, which is defined by

$$x=a\cos\theta(1+0.5\cos\theta),\quad y=b\sin\theta(1+0.8\sin\theta). \tag{20}$$

In the case of $b/a=0.5$, the configuration is shown in Fig. 5(c).

Similar to the elliptic notch case, the degenerate scales are expressed as

$$\lambda_1=f_1(b/a),\quad \lambda_2=f_2(b/a)\quad \text{(using the kernel } U_{ij}^{*1}(\xi,x)), \tag{12c}$$

$$\lambda_1=g_1(b/a),\quad \lambda_2=g_2(b/a)\quad \text{(using the kernel } U_{ij}^{*2}(\xi,x)). \tag{19c}$$

The computed results for $\lambda_1=f_1(b/a)$, $\lambda_2=f_2(b/a)$, $\lambda_1=g_1(b/a)$ and $\lambda_2=g_2(b/a)$ are listed in Table 4. Similar characters as mentioned in the Example 3.1 can be found from the tabulated results.

Similar to Eq. (17), the eigenfunctions are expressed as

$$p_1=p_1(b/a,\theta),\quad p_2=p_2(b/a,\theta). \tag{21}$$

Under the following conditions: (a) $\nu=0.3$, (b) for three particular cases: $b/a=0.5$ (with $a=\lambda_1=1.392297$), $b/a=0.7$ (with $a=\lambda_1=1.175415$) and $b/a=0.9$ (with $a=\lambda_1=1.028311$), the computed results are plotted in Fig. 6. From plotted results, it is see that in the case of the first eigenvalue $a=\lambda_1$, generally, $|p_1|>|p_2|$. Some peak stresses have been found from Fig. 6, for example, $p_1|_{b/a=0.5}=2.101$, $p_1|_{b/a=0.7}=2.883$, and $p_1|_{b/a=0.9}=3.229$, at near $\theta=216^\circ$. These peak stresses may be caused by a higher curvature at some point on the contour (indicated by point G in Fig. 5(c)).

The merit of the obtained solution $p_1=p_1(b/a,\theta)$ and $p_2=p_2(b/a,\theta)$ is as follows. For $b/a=0.5$ case, if one

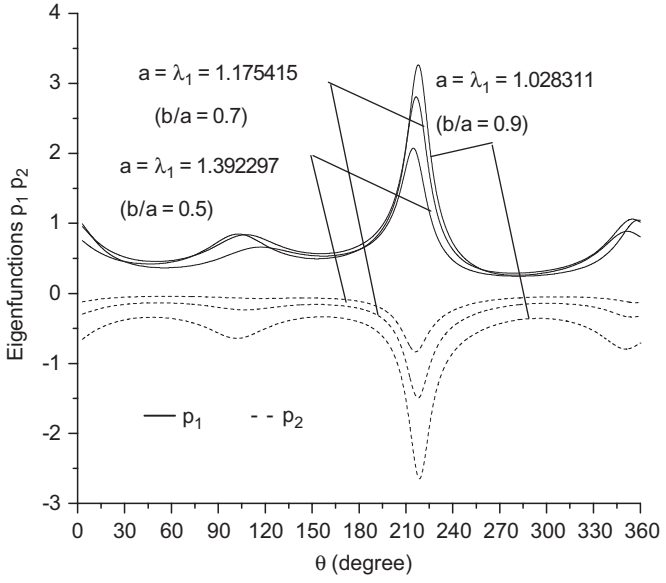

Fig. 6. Eigenfuctions $p_1(b/a,\theta)$, $p_2(b/a,\theta)$ for a complicated notch for three cases: (a) $a=\lambda_1=1.392297$ (with $b/a=0.5$), (b) $a=\lambda_1=1.175415$ (with $b/a=0.7$) and (c) $a=\lambda_1=1.028311$ (with $b/a=0.9$) (see Fig. 5(c) and Eq. (21)).

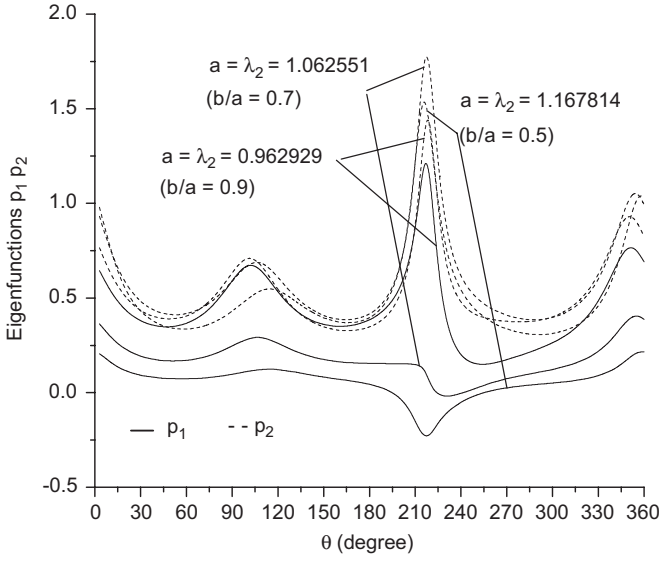

Fig. 7. Eigenfuctions $p_1(b/a,\theta)$, $p_2(b/a,\theta)$ for a complicated notch for three cases (a) $a=\lambda_2=1.167814$ ($b/a=0.5$), (b) $a=\lambda_2=1.062551$ ($b/a=0.7$) and (c) $a=\lambda_2=0.962929$ ($b/a=0.9$) (see Fig. 5(c) and Eq. (21)).

substitutes the relevant eigenvalue $a = \lambda_1 = 1.392297$ and the solution $p_1 = p_1(b/a, \theta)$ and $p_2 = p_2(b/a, \theta)$ (shown in Fig. 6 for the case of $b/a = 0.5$) into the left-hand side of homogenous equation (8) (or into its discrete form shown by Eq. (10)), the Eq. (8) is satisfied. Alternatively speaking, the homogenious equation has a non-trivial solution $p_1 = p_1(b/a, \theta)$ and $p_2 = p_2(b/a, \theta)$ when the degenerate size ($a = \lambda_1 = 1.392297$) is reached. Naturally, a non-trivial solution for the homogeneous equation will cause an improper solution for the non-homogenous equation.

Meantime, under the following conditions: (a) $v = 0.3$, (b) for three cases: $b/a = 0.5$ (with $a = \lambda_2 = 1.167814$), $b/a = 0.7$ (with $a = \lambda_2 = 1.062551$) and $b/a = 0.9$ (with $a = \lambda_2 = 0.962929$), the computed results are plotted in Fig. 7. From plotted results, it is seen that in the case of the second eigenvalue $a = \lambda_2$, generally, $|p_1| < |p_2|$. The merit for the obtained results in Fig. 7 is similar to the previously mentioned case.

4. Conclusions

It is well known that the natural vibration of a bar can be reduced to a problem for finding eigenvalues and eigenfunctions. The eigenvalue in the problem is the natural vibration frequency, and the eigenfunction is the vibration mode. Similar idea is developed in the present study. However, if the problem is formulated in the form of integral equation shown by Eq. (8), we cannot obtain useful results from the formulation since the equation is too complicated. The discretization of the integral equation in the form of Eqs. (9) and (10) is an essential step in the present study. From the dependence of det (**U**) with respect to the size a, the eigenvalues and the eigenfunctions in the problem can be evaluated immediately.

The merit of the present study is emphasized here once more. For a real displacement boundary value problem, from Eq. (7) the governing equation can be written as follows:

$$\int_\Gamma U_{ij}^{*1}(\xi, x) p_j(x)\, \mathrm{d}s(x) = q_i(\xi), \quad (i = 1, 2,\ \xi \in \Gamma). \tag{22}$$

The functions $q_i(\xi)$ $(i = 1, 2)$ are simply obtained from a substitution of the given displacements into the left-hand side of Eq. (7). Alternatively, Eq. (22) can be rewritten in a discrete form

$$U\tilde{p} = q, \tag{22a}$$

where **U** is a matrix after discritization of the kernel $U_{ij}^{*1}(\xi, x)$, and $\tilde{p}$ and $\boldsymbol{q}$ are two vectors from the functions $p_j(x)$ and $q_i(\xi)$.

In addition, the relevant homogenous equations can be written as follows:

$$\int_\Gamma U_{ij}^{*1}(\xi, x) p_j(x)\, \mathrm{d}s(x) = 0, \quad (i = 1, 2,\ \xi \in \Gamma), \tag{23}$$

$$U\tilde{p} = 0. \tag{23a}$$

As mentioned previously, for the elliptic notch with $b/a = 0.5$, there are two eigenvalues, $a = \lambda_1 = 1.463102$ and $a = \lambda_2 = 1.215765$, and relevant eigenfunctions p_1, p_2 (shown in Figs. 3 and 4 for the case of $\beta = 0^\circ$). Naturally, a non-trivial solution for the homogeneous equations (23) or (23a) will cause an improper solution for the non-homogenous equations (22) and (22a). That is to say, in order to avoid obtaining an improper solution for Eq. (22), one cannot adopt $a = \lambda_1 = 1.463102$ or $a = \lambda_2 = 1.215765$ in a real computation.

Obviously, the mentioned analysis can find its practical usage in engineering. For example, let us perform a stress analysis for an elliptic notch with size $a = 1.463$ m and $b = 0.5a$. From Table 1 we know that for the ratio $b/a = 0.5$ there are two eigenvalues $a = \lambda_1 = 1.463102$ and $a = \lambda_2 = 1.215765$. Clearly, in order to avoid obtaining an improper solution, we cannot use the value $a = 1.463$ (means $a = 1.463$ m) and $b = 0.5a$. Instead, we have to use, for example, the value $a = 146.3$ (means $a = 146.3\,\mathrm{cm} = 1.463$ m) and $b = 0.5a$. Computed results prove that if one assumes $a \geqslant 1.1\lambda_1$ or $a \leqslant 0.9\lambda_2$ in computation, the improper solution can be avoided properly.

Acknowledgment

The project is supported by the National Natural Science Foundation of China.

Appendix A

The following analysis depends on the complex variable function method in plane elasticity [11]. In the method, the stresses $(\sigma_x, \sigma_y, \sigma_{xy})$, the resultant forces (X, Y) and the displacements (u, v) are expressed in terms of two complex potentials $\phi(z)$ and $\psi(z)$ such that

$$\sigma_x + \sigma_y = 4\,\mathrm{Re}\,\phi'(z),$$

$$\sigma_y - \sigma_x + 2\mathrm{i}\sigma_{xy} = 2[\bar{z}\phi''(z) + \psi'(z)], \tag{A.1}$$

$$f = -Y + \mathrm{i}X = \phi(z) + z\overline{\phi'(z)} + \overline{\psi(z)}, \tag{A.2}$$

$$2G(u + \mathrm{i}v) = \kappa\phi(z) - z\overline{\phi'(z)} - \overline{\psi(z)}, \tag{A.3}$$

where $z = x + \mathrm{i}y$ denotes complex variable, G is the shear modulus of elasticity, $\kappa = (3 - v)/(1 + v)$ is for the plane stress problems, $\kappa = 3 - 4v$ is for the plane strain problems, and v is the Poisson's ratio. In the present study, the plane strain condition is assumed thoroughly.

The fundamental stress field is defined by a concentrated force (P_x, P_y) applied at the point $z = t$ of an infinite plate (Fig. 1(a)). The relevant complex potentials are defined by [11]

$$\phi(z) = F\ \ln(z - t), \quad \psi(z) = -\kappa\bar{F}\ \ln(z - t) - \frac{F\bar{t}}{z - t}, \tag{A.4}$$

where

$$F = -\frac{P_x + \mathrm{i}P_y}{2\pi(\kappa + 1)}. \tag{A.5}$$

Let $\{f\}_{in} = \{-Y + iX\}_{in}$ denotes the increase of the function $f = -Y + \mathrm{i}X$ in Eq. (A.2) when a moving point is going forward in the anticlockwise direction around the point $z = t$. From this definition, we have

$$\{f\}_{in} = \{-Y + iX\}_{in} = P_y - iP_x, \text{ or } \{Y\}_{in} = -P_y \text{ and } \{X\}_{in} = -P_x. \tag{A.6}$$

The loading condition is indicated in Fig. 1(a). From the suggested complex potentials shown by Eq. (A.4), the kernel $U_{ij}^{*1}(\xi, x)$ shown by Eq. (6) can be obtained immediately.

By using an equation for evaluating a MWDI [12,13], we can prove the following equality

$$D_1(CR) = -\int_{CR} P_{ij}^{*}(\xi, x)u_j(x)\,\mathrm{d}s(x) + \int_{CR} U_{ij}^{*1}(\xi, x)p_j(x)\,\mathrm{d}s(x) = 0. \tag{A.7}$$

References

[1] Rizzo RL. An integral equation approach to boundary value problems in classical elastostatics. Quart J Appl Math 1967;25:83–95.

[2] Cruse TA. Numerical solutions in three-dimensional elastostatics. Int J Solids Struct 1969;5:1259–74.

[3] Brebbia CA, Tells JCF, Wrobel LC. Boundary element techniques—theory and application in engineering. Heidelberg: Springer; 1984.

[4] Cheng AHD, Cheng D S. Heritage and early history of the boundary element method. Eng Anal Boundary Elements 2005;29:286–302.

[5] Chen JT, Lee CF, Chen IL, Lin JH. An alternative method for degenerate scale problems in boundary element methods for the two-dimensional Laplace equation. Eng Anal Boundary Elements 2002;26:559–69.

[6] Chen JT, Lin JH, Kuo SR, Chiu YP. Analytical study and numerical experiments for degenerate scale problem in boundary element method using degenerate kernels and circulants. Eng Anal Boundary Elements 2001;25:819–28.

[7] Chen JT, Wu CS, Chen KH, Lee YT. Degerate scale for the analysis of circular thin plate using the boundary integral equation method and boundary element methods. Comput Mech 2006;36: 33–49.

[8] He WJ, Ding HJ, Hu HC. Non-equivalence of the conventional boundary integral formulation and its elimination for plane elasticity problems. Comput Struct 1996;59:1059–62.

[9] He WJ, Ding HJ, Hu HC. Degenerate scales and boundary element analysis of two dimensional potential and elasticity problems. Comput Struct 1996;60:155–8.

[10] Chen JT, Kuo SR, Lin JH. Analytical study and numerical experiments for degenerate scale problems in the boundary element method of two-dimensional elasticity. Int J Numer Meth Eng 2002; 54:1669–81.

[11] Muskhelishvili NI. Some basic problems of mathematical theory of elasticity. Groningen: Noordhoof; 1959.

[12] Buecker HF. Field singularities and related integral representation. In: Sih GC, editor. Mechanics of fracture, vol. 1. Leyden: Noordhoff; 1973. p. 239–314.

[13] Chen YZ. Analysis of L-integral and theory of the derivative stress field in plane elasticity. Inter J Solids Struct 2003;40:3589–602.